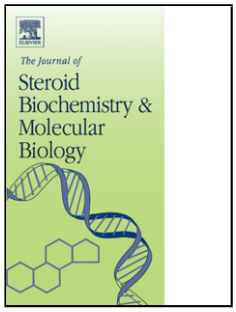

Title: Differential modulation of hepatitis C virus replication and innate immune pathways by synthetic calcitriol-analogs

Authors: Maged Saleh, Christoph Welsch, Chengcong Cai, Claudia Döring, Jérôme Gouttenoire, Judith Friedrich, Katrin Haselow, Christoph Sarrazin, Klaus Badenhoop, Darius Moradpour, Stefan Zeuzem, Sabrina Rueschenbaum, Christian M. Lange

PII: S0960-0760(18)30202-4
DOI: https://doi.org/10.1016/j.jsbmb.2018.06.008
Reference: SBMB 5166

To appear in: *Journal of Steroid Biochemistry & Molecular Biology*

Received date: 27-10-2017
Revised date: 10-5-2018
Accepted date: 6-6-2018

Please cite this article as: Saleh M, Welsch C, Cai C, Döring C, Gouttenoire J, Friedrich J, Haselow K, Sarrazin C, Badenhoop K, Moradpour D, Zeuzem S, Rueschenbaum S, Lange CM, Differential modulation of hepatitis C virus replication and innate immune pathways by synthetic calcitriol-analogs, *Journal of Steroid Biochemistry and Molecular Biology* (2018), https://doi.org/10.1016/j.jsbmb.2018.06.008

Differential modulation of hepatitis C virus replication and innate immune pathways by synthetic calcitriol-analogs

Running title: Calcitriol derivatives and hepatocellular VDR signaling

Maged Saleh[a]*, Christoph Welsch[a]*, Chengcong Cai[a], Claudia Döring[b], Jérôme Gouttenoire[c], Judith Friedrich[a], Katrin Haselow[a], Christoph Sarrazin[a,d], Klaus Badenhoop[a], Darius Moradpour[c], Stefan Zeuzem[a], Sabrina Rueschenbaum[a], Christian M. Lange[a,#]

[a]Department of Medicine 1, J.W. Goethe University Hospital, D-60590 Frankfurt a.M., Germany

[b] Senckenberg Institute of Pathology, Goethe University Hospital, D-60596 Frankfurt a. M., Germany

[c]Division of Gastroenterology and Hepatology, University Hospital Lausanne, CH-1011 Lausanne, Switzerland

[d]Medical Department II Gastroenterology, Hepatology, Infectiology, Diabetology, St. Josefs-Hospital, D-65189 Wiesbaden, Germany

[#]Corresponding author at: Department of Gastroenterology and Hepatology, University Hospital Essen, Hufelandstr. 55, D-45137 Essen, Germany. Phone +49 201 723 3612, Fax +49 201 723 5745. E-Mail address: christian.lange@uk-essen.de (C.M. Lange, current address).

Footnotes

[*]These authors have contributed eaqually to this work.

Graphical abstract

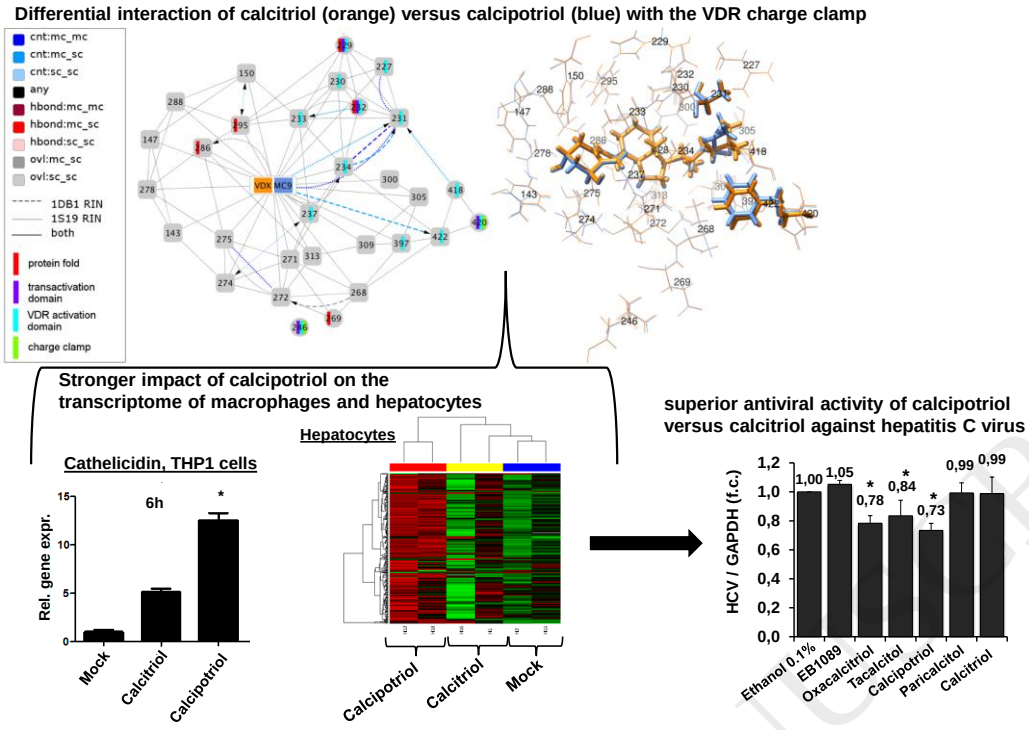

Highlights

- Identification of calcitriol-analogs with intrinsic inhibitory effects against HCV replication.
- Distinctive interactions of calcipotriol as the lead analog with critical VDR regulatory
- residues Differential impact of calcipotriol on innate immune pathways

ABSTRACT

Background and Aims: Vitamin D signaling is involved in infectious and non-infectious liver diseases, yet the natural vitamin D metabolites are suboptimal therapeutic agents. In the present study, we therefore aimed to explore the potential and mechanism of selected calcitriol analogs to regulate the hepatocellular transcriptome and to inhibit hepatitis C virus (HCV) in comparison with calcitriol.

Methods: Human hepatoma cell lines and primary human macrophages were stimulated with calcitriol and selected calcitriol analogs. The effect of calcitriol and its derivatives on

hepatocellular gene expression and vitamin D receptor (VDR) signaling as well as on replication of HCV were assessed by quantitative PCR, microarray analyses and *in silico* analyses of ligand-VDR complexes.

Results: The structurally related vitamin D analogs calcipotriol and tacalcitiol, but not calcitriol itself, suppressed HCV replication in a VDR-dependent manner. Using a residue-interaction network approach we outline structural and functional differences between VDR-ligand complexes. In particular we find characteristics in the VDR structure bound to calcipotriol with distinct local residue interaction patterns that affect key functional residues that pertain to the VDR charge clamp, H397 and F422, a VDR regulatory element for interaction with co-activators and -repressors. As a consequence, we show calcipotriol in comparison to calcitriol to induce stronger regulatory actions on the transcriptome of hepatocytes and macrophages including key antimicrobial peptides.

Conclusion: Calcipotriol induces local structure rearrangements in VDR that could possibly translate into a superior clinical potential to execute important non-classical vitamin D effects such as inhibition of HCV replication.

Abbreviations

HCV, hepatitis C virus; VDR, vitamin D receptor; IFN-α, interferon-α; ISG, interferon-stimulated gene; LBD, ligand-binding domain; CoA, coactivator; CoR, corepressor; IGF-2,insulin-like growth factor 2; IL-32, interleukin-32; CCL20, C-C motif chemokine 20; HSPA8, heat shock protein family A member 8; TGF-β, transforming growth factor-β

Key words: vitamin D receptor, calcipotriol, cathelicidin, hepatitis C, macrophage

1. Introduction

Vitamin D deficiency and functional polymorphisms in genes involved in vitamin D signaling are associated with the occurrence, natural course, and treatment outcome of various diseases including infections with chronic hepatitis B or C virus, Mycobacterium tuberculosis, or influenza virus [1-7]. Furthermore, extensive *in vitro* and animal studies have shown that vitamin D is a potent modulator of numerous innate and adaptive immunity pathways[8-10]. Yet, the translation of these data to a successful clinical application of vitamin D to prevent or to treat infectious diseases is still in its infancy, although preliminary data indicate a possible benefit of vitamin D supplementation for example during treatment of lung tuberculosis or influenza [11, 12]. These difficulties may be partially explained by the complexity and pleiotropy of vitamin D signaling, in which the optimal strategy for therapeutic interventions is not yet defined. Furthermore, these so called non-classical vitamin D effects (in contrast to the classical role, calcium homeostasis), are partially exerted by supraphysiological doses of calcitriol, which bear a substantial risk of hypercalcemia, whereas calcitriol analogues may be effective at lower doses with a lower risk of hypercalcemia [13-15].

Cholecalciferol, the precursor of vitamin D, is hydroxylated in the liver at position 25 to 25-hydroxyvitamin D 25(OH)D_3 and subsequently in the kidney at position 1 to 1,25-dihydroxyvitamin D (1,25(OH_2)D_3, = calcitriol), the bioactive vitamin D metabolite [16, 17]. Because of its long half-life and reliable quantification assays, 25(OH)D_3 is usually determined to assess the patients vitamin D status [16, 17]. Most experimental therapeutic approaches in infectious (and other) diseases have thus far been based on assessment of 25(OH)D_3 serum concentration and on supplementation of its precursor cholecalciferol [16, 17]. Overall, therapeutic strategies that target directly the vitamin D receptor (VDR) might be superior to cholecalciferol supplementation, especially in clinical scenarios in which a rapid modulation of VDR signaling would be required. The clinical usage of calcitriol, however, is hampered by a relatively high risk of side-effects, in particular hypercalcemia. Therefore, several calcitriol analogs have been

developed which bind and activate the VDR as well, but which have a lower impact on calcium metabolism than calcitriol [18].

Previously, we have shown that calcitriol potentiates the antiviral effect of interferon-α (IFN-α) via a molecular crosstalk between VDR and Jak-STAT signaling cascades[19]. Because of the clinical limitations of calcitriol therapy described above, we here aimed to explore the possible therapeutic effects of calcitriol analogs on hepatitis C virus (HCV), a highly relevant causative agent of chronic hepatitis in word-wide populations. As described in the following, our study reveals fundamental differences between calcitriol *versus* selected calcitriol analogs with respect to hepatocellular VDR signaling and downstream suppression of HCV and induction of mediators of innate immunity.

2. Materials and Methods

2.1 Cell culture, subgenomic replicons, plasmids, reagents

Huh-7.5 human HCC cells and the subgenomic replicon construct pCon1/SG-Neo(I)/AflII (Con1 strain, genotype 1b) [20] were provided by Charles M. Rice (The Rockefeller University, New York, NY), and cultured as described previously [19]. Subgenomic replicon construct pFK_i389NeoNS3-39_JFH_dg (JFH1 strain, genotype 2a) were provided by Ralf Bartenschlager (University of Heidelberg, Heidelberg, Germany) [21]. Wild-type constructs of VDR (pCMV-FLAG-VDR[22]) and, SRC-1 (pSG5-SRC-1-FLAG)[23] were provided by Klaus Roemer (University Hospital Saarland, Germany) and Nicolas Mitsiades (Baylor College of Medicine, TX), respectively. For pCMV-FLAG-VDR and pSG5-SRC-1-FLAG, plasmid transfection was carried out for Huh-7.5 cells using X-tremeGENE HP DNA transfection reagent (Roche Diagnostics, Mannheim, Germany). THP-1 cells were cultured in RPMI 1640 medium (Life Technologies, Carlsbad, CA) containing 10% heat-inactivated FCS and were differentiated to macrophage-like cells in PMA (Sigma-Aldrich, Darmstadt, Germany) at a

concentration of 50 nmol/ml for 72 h. Human monocyte-derived macrophages (MDMs) were generated from buffy coats from healthy donors (German Red Cross Blood Donor Service Baden-Württemberg and Hesse, Frankfurt, Germany). To this end, peripheral blood mononuclear cells (PBMCs) were separated by density gradient using Ficoll-Plaque Plus (GE Healthcare, Little Chalfont, UK). Subsequently, $CD14^+$ monocytes were isolated using CD14 microbeads (Miltenyi Biotec, Bergisch Gladbach, Germany) and cultivated in RPMI with 10% heat-inactivated FBS, 1% penicillin-streptomycin and 20ng/ml rhM-CSF (Peprotech, Rocky Hill, NJ) for 6 days to differentiate into MDMs. Calcitriol was purchased from Sigma-Aldrich. The calcitriol analogs EB1089, oxacalcitriol, tacalcitol, and calcipotriol, as well as the HCV inhibitors daclatasvir and lomibuvir, were purchased from SelleckChem (Houston, TX). The calcitriol analog paricalcitol was provided by AbbVie (Lake Bluff, IL). Calcitriol and its analogs were reconstituted in 100% ethanol, and applied to cells in a final volume corresponding to 0.1% ethanol. Control groups were also cultured in the presence of 0.1% ethanol (mock), unless stated otherwise. Human IFN-α2a was provided by Roche (Basel, Switzerland). Cytotoxicity was assessed using the WST-1 Cell Proliferation Reagent from Takara Bio (Kusatsu, Shiga, Japan).

2.2 BrdU Proliferation assay

For assessment of cellular proliferation, BrdU (Sigma-Aldrich) was added at a final concentration of 5µg/ml, followed by trypsinization and fixation of the cells with 70 % ethanol. DNA was denaturated with 2 N HCl/0.5% Triton X-100 for 30 min and neutralized with 0.1 M sodium tetraborate. Afterwards, cells were pelleted and washed with PBS/ 1% BSA, followed by incubation with clone 3D4 of FITC anti-BrdU antibody (BioLegend, San Diego, CA). Cells were then pelleted and resuspended in PBS containing 20 µg/ml RNase A and 20 µg/ml propidium iodide. Finally, cells were analyzed by flow cytometry using a FACS Calibur (BD Biosciences, Franklin Lakes, NJ) and version 7.6 of FlowJo software (FlowJo LLC,

Ashland, OR) to generate graphical plots. The percentage of S-Phase BrdU positive cells were analyzed in the FL2-H (PI Staining) x FL1-H (BrdU staining) plot.

2.3 Reverse transcription, quantitative PCR and agarose gel electrophoresis

Total RNA extraction was performed using the RNeasy Mini Kits for mRNA (Qiagen, Hilden, Germany). Reverse transcription of mRNA was performed using the PrimeScript RT reagent kit (Takara Bio). Quantitative real-time PCR was performed using a QuantiTect SYBR Green PCR kit (Qiagen, Hilden, Germany). Primers for amplification of GAPDH mRNA and HCV RNA [24] as well as for 1,25-$(OH)_2D_3$ 24-hydroxylase (*CYP24A1*) and interferon-stimulated gene (ISG) mRNAs (IFI27L, IFI44L, ISG15)[19] were previously described. Additional primers are listed in SI-Table 1. For DNA gel electrophoresis, 1% ethidium bromide-containing agarose gel was used. DNA was mixed with 1/3 volume of 6X Gel DNA loading dye (Thermo Scientific, Waltham, MA), then loaded onto the solidified agarose gel for separation at 100 volts. UV detection of the DNA bands was carried out using ChemiDoc XRS imaging system (Bio-rad, Hercules, CA).

2.4 Transcriptome analysis

RNA isolation, cRNA generation and fragmentation, as well as hybridization to GeneChip HG-U133-Plus2.0 arrays (Affymetrix, Santa Clara, CA) were described previously[25]. The gene expression dataset is available at http://www.ncbi.nlm.nih.gov/geo/ (accession no. GSE106234). Bioinformatics and statistical analyses were performed using GeneSpring Version 7.3.1 software (Agilent Technologies, Santa Clara, CA) with GC-RMA preprocessing of the raw expression data (CEL files) and with the computing environment R, respectively, as described previously[25].

2.5 Co-immunoprecipitation

Huh-7.5 cells were harvested and lysed, followed by collection of protein by centrifugation. For each sample, 4 μg of anti-VDR antibody were crosslinked to 50 μL of Dynabeads Protein

G (Thermo Scientific), followed by incubation of lysates with the bead-antibody complex. The desired antibody-antigen complexes were finally eluted from the beads and anaylsis was carried out by FLAG-immunoblotting.

2.6 Immunoblotting

Immunoblotting was performed as described previously [19]. Mouse monoclonal antibody against VDR (sc-13133) and β-actin (AC-15) were purchased from Santa Cruz Biotechnology (Dallas, TX) and Sigma-Aldrich, respectively. Monoclonal antibody against HCV NS5B (12B7) was described earlier[26]. Rabbit monoclonal antibody against FLAG M2 tag was purchased from Cell Signaling Technology (Danvers, MA).

2.7 Gene silencing

Gene silencing was performed as described[19] using the following pre-designed small interfering RNAs (siRNAs) from Applied Biosystems (Foster City, CA): s1477 or s14779 for VDR, or non-targeting control siRNA.

2.8 Structure data

We used experimental protein structure information from the Protein Databank RCSB PDB[27] for 3D structure analysis and residue-interaction networks (RINs). Two alternative structures of the ligand-binding domain (LBD) of the nuclear receptor for vitamin D (VDR) were identified and downloaded from PDB, bound either to the natural ligand calcitriol or the synthetic analog calcipotriol (1DB1[28] or 1S19[29], respectively). The PDB entry 1DB1 comprises a 1.8 A resolution crystal structure of an active conformation of the complex between a VDR-LBD construct lacking the highly variable VDR-specific insertion domain and calcitriol ($1\alpha,25(OH)_2D_3$). PDB-1S19 is a crystal structure of VDR-LBD bound to the vitamin D agonist calcipotriol that is characterized by side chain modifications compared to calcitriol.

2.9 Residue interaction data

For both structures, we created a *residue interaction network* (RIN) using the RINerator tool[30]. To this end, hydrogens are first added to the 3D protein structure using the Reduce tool[31]. Then contacts on the van-der-Waals (vdW) surface of each atom are sampled by the Probe tool[32] and are finally summarized into residue interactions by RINerator. In the resulting network, nodes represent protein residues and edges indicate non-covalent residue interactions between these residues. The following interaction types are identified: van-der-Waals contacts (cnt), hydrogen bonds (hbond), overlaps of van-der-Waals radii (ovl), and combined (any of the previous three). We also distinguish between two types of interacting atoms: main chain (mc) and side chain (sc). The RINs and additional data associated with them can be loaded and visualized in Cytoscape using the RINalyzer and structureViz2 apps[33]. In particular, we enriched the networks with functional site annotations. PyMOL and CHIMERA were used for 3D protein structure analysis and visualization.

2.10 Selection of functional sites

For functional annotation of nodes in the RIN, we reviewed available literature on VDR functional sites[29, 34]. Residues in the RIN previously identified to pertain to different VDR function were grouped as follows: Protein fold ("sandwitch structure"): residues 154, 229, 232, 269, 279, 286, 295, 337, 343, 394; VDR activation domain: residues 195-238, 246, 397, 417-423; VDR “charge clamp”: residues 246, 420 ; Transactivation domain: residues 229, 232, 236, 246, 420.

3 Results

3.1 Selected calcitriol analogs have an intrinsic inhibitory effect on HCV replication

Previously, we have shown that calcitriol enhances the antiviral activity of IFN-α via a Jak-STAT / VDR signalling crosstalk[19]. We therefore tested the ability of the calcitriol analog calcipotriol to enhance IFN-α signalling in Huh-7.5 cells harbouring subgenomic HCV genotype 1b replicons. As described previously[19], the presence of VDR on the mRNA and

protein level could be confirmed in these cell lines (Fig. 1A, B). As shown in Fig. 1C, administration of calcipotriol plus IFN-α resulted in a significantly stronger inhibition of HCV replication, and in a moderately (non-significant) increased induction of interferon-stimulated genes (ISGs) ISG-15 and IFL-27 (Fig. 1D) than administration of IFN-α alone. Interestingly, treatment with calcipotriol alone resulted in a reduction of HCV replication as well (Fig. 1C), a phenomenon which we have not observed for the natural vitamin D metabolite calcitriol [19].

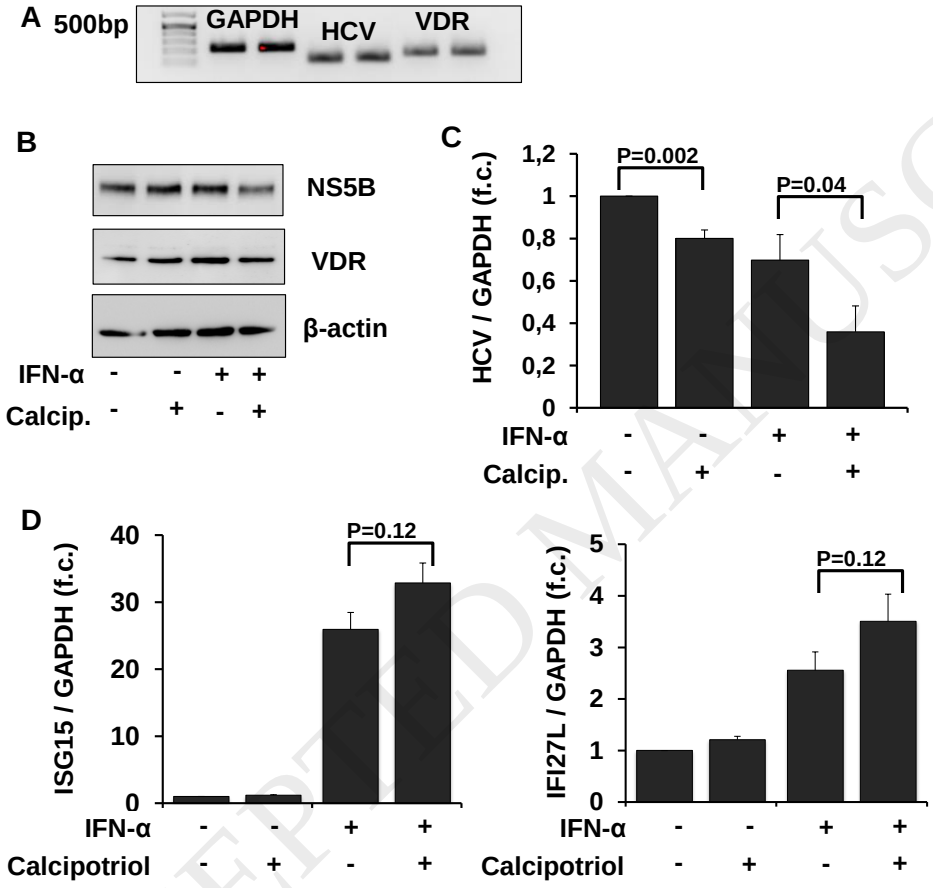

Fig. 1. Calcipotriol increases the antiviral activity of IFN-α. (A) Validation of the PCR method. mRNA of Huh-7.5 cells harboring subgenomic HCV genotype 1b replicons was extracted and subjected to quantitative PCR of GADH, HCV, and VDR cDNA. After 40 cyles, the PCR products of two technical replicates were loaded on an agarose gel. (B) Huh-7.5 cells harboring subgenomic HCV genotype 1b replicons were treated with IFN-α (10 IU/mL) or mock in combination with or without calcipotriol (10 nM) after a pretreatment period of 6 hours, with or without calcipotriol. Protein levels of HCV NS5B, VDR and ß-actin were analyzed by Western blot after 24h of combination therapy. (C)

Huh-7.5 cells harboring subgenomic HCV genotype 1b replicons were treated with IFN-α (10 IU/mL) or mock in combination with or without calcipotriol (10 nM) after a pretreatment period of 6 hours with or without calcipotriol. HCV RNA levels relative to GAPDH mRNA were assessed after 24h of treatment. Standard deviations of three independent experiments are shown. *$P < 0.05$. (D) Huh-7.5 cells harboring subgenomic HCV genotype 1b replicons were treated for 6 hours with calcipotriol (10 nM) and IFN-α (10 IU/mL) after a pretreatment period of 6 hours with or without calcipotriol, as indicated. mRNA expression of the indicated ISGs was normalized to GAPDH mRNA and expressed as fold induction relative to mock treated cells. Results are from three independent experiments. f.c., fold change.

Next, we screened a panel of synthetical calcitriol analogs for intrinsic antiviral activity. As excpected, calcitriol, as well as its structurally closely related analogs EB1089 and paricalcitol, had no effect on HCV replication when administered alone (Fig. 2A). In contrast, the structurally related calcitriol analogs oxacalcitriol, calcipotriol and tacalcitol significantly suppressed replication of HCV genotype 1b replicons (Fig. 2A). From these screening experiments, we selected calcipotriol as a lead compound for subsequent experiments. Calcipotriol inhibited HCV replication in a time-dependent manner, and even picomolar doses (which are comparable to plasma concentrations of calcitriol in humans) of calcipotriol were sufficient for inhibition of HCV replication at the mRNA (Fig. 2B) and protein level (Fig. 2C). Calcipotriol also inhibited replication of a HCV genotype 2 replicon (Fig. 2D), although the effect appeared to be somewhat less pronounced compared to HCV genotype 1b (Fig. 2A). Of potential clinical importance, co-administration of calcipotriol in picomolar ranges increased the antiviral effect of lomibuvir or daclatasvir, as shown by qPCR for two clinically effective inhibitors of the HCV NS5B and NS5A proteins, respectively (Fig. 2E and F). Of note, neither the natural VDR agonist calcitriol nor calcipotriol or other calcitriol analogs affected viability and proliferation of Huh-7 cells (Fig. 3).

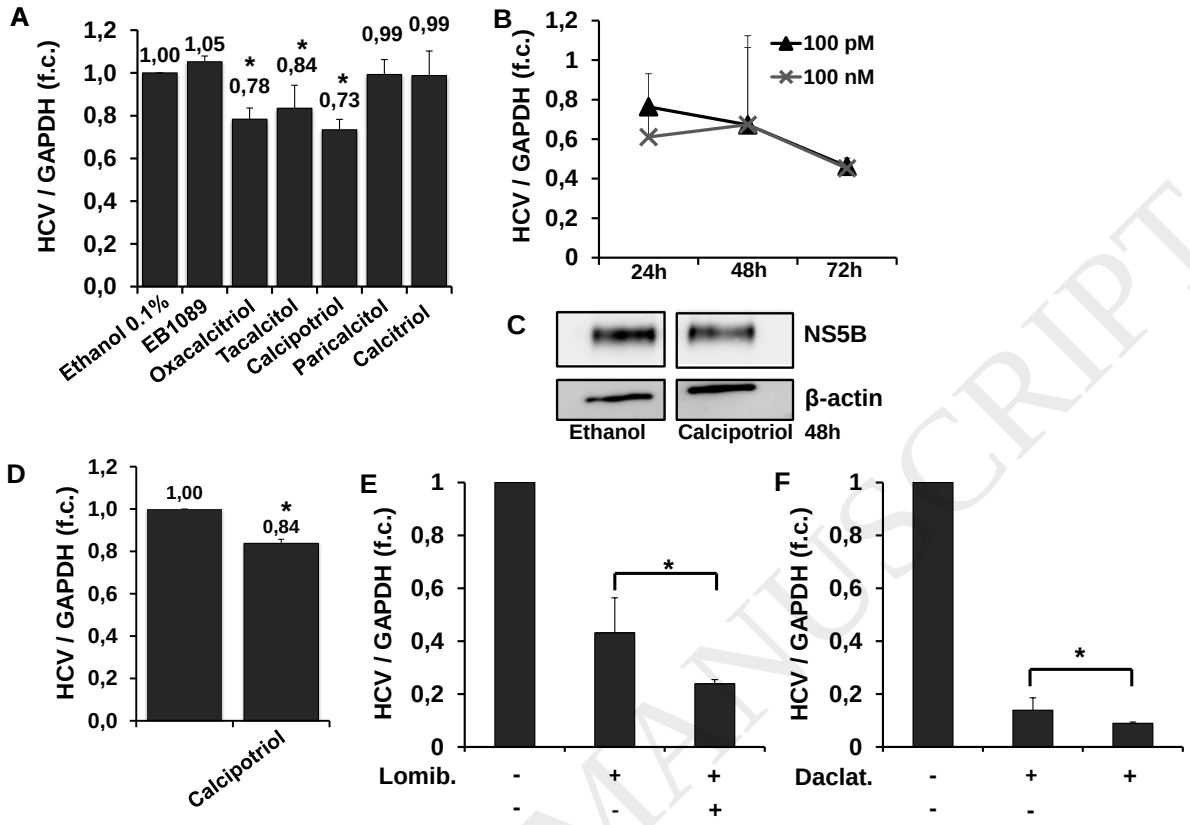

Fig. 2. Screening calcitriol analogs for direct antiviral activity. (A) Huh-7.5 cells harboring subgenomic HCV genotype 1b replicons were treated with mock (0.1% ethanol), calcitriol (10nM) or the indicated calcitriol analogs (10 nM). HCV RNA levels relative to GAPDH mRNA were assessed after 24 hours of treatment and expressed as fold change relative to mock treated cells. Standard deviations of six independent experiments are shown. **P* < 0.05. f.c., fold change. (B) Huh-7.5 cells harboring subgenomic HCV genotype 1b replicons were treated with mock (0.1% ethanol), or calcipotriol for 24-72 hours. HCV RNA levels relative to GAPDH mRNA were assessed and expressed as fold change relative to mock treated cells. Standard deviations of three independent experiments are shown. (C) Immunoblot analyses for HCV NS5B protein and β-actin was performed for Huh-7.5 cells harboring subgenomic HCV genotype 1b replicons after 48 hours of treatment with 100 pM calcipotriol. (D) Huh-7.5 cells

harboring subgenomic HCV genotype 2a replicons were treated with 10 nM calcipotriol for 24 hours. HCV RNA levels normalized to GAPDH were assessed relative to mock treated cells. (E and F) Huh-7.5 cells harboring subgenomic HCV genotype 1b replicons were treated with the direct-acting antivirals (E) Lomibuvir (10 nM) and (F) daclatasvir (5 pM) combination with or without calcipotriol (100 pM). HCV RNA levels relative to GAPDH mRNA were assessed after 24 hours of treatment and expressed as fold change relative to mock treated cells. Standard deviations of three independent experiments are shown. *$P < 0.05$. f.c., fold change.

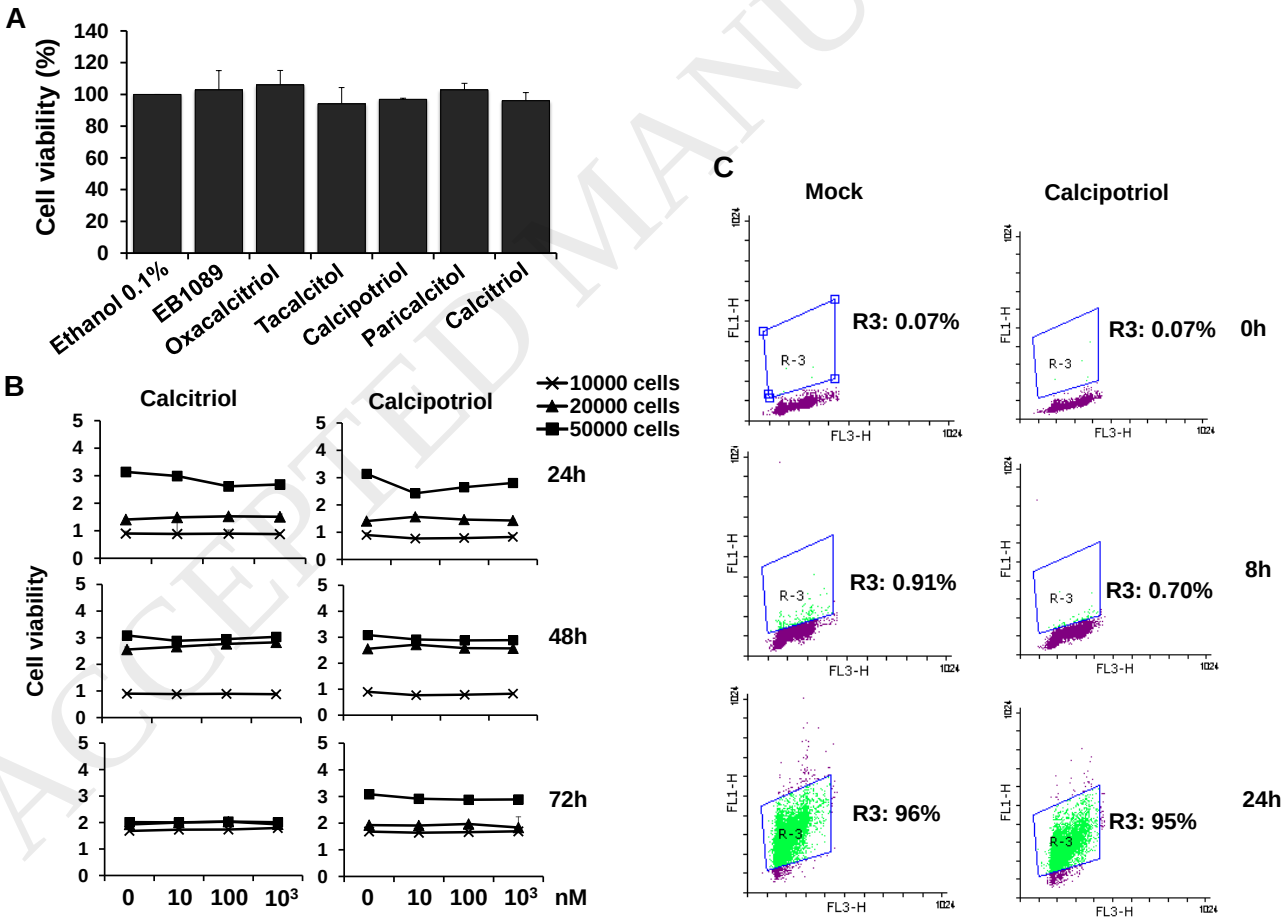

Fig. 3. Cytotoxicity of calcitriol analogs. (A) WST-1 assay for cells treated with calcitriol analogs. Huh-7.5 cells harboring subgenomic HCV genotype 1b replicons were cultured for 24

hours in the presence of 10 nM calcitriol as well as 10 nM of the calcitriol-analogs. Cytotoxicity was assessed using WST-1 assay at a seeding density 20,000 cells per well in 96-well plates. (B) WST-1 assay for calcitriol- and calcipotriol-treated cells. Huh-7.5 cells harboring subgenomic HCV genotype 1b replicons were cultured at seeding densities of 10,000, 20,000 and 50,000 cells per well for 24, 48 and 72 hours in the presences of 10, 100 and 10^3 nM of calcitriol or calcipotriol in 96-well plates. Absorbance readings ($A_{450nm} - A_{690nm}$) of calcitriol- or analogs-treated cells were compared to mock (0.1% ethanol) treated cells to calculate the respective cell viability percentage. Standard deviations of six independent experiments are shown. (C) BrdU incorporation for mock- and calcipotriol-treated cells (10^3 nM). Huh-7.5 cells harboring subgenomic HCV genotype 1b replicons were exposed to BrdU and cultured for 0, 8 or 24 hours.

3.2 The antiviral effects of calcipotriol are VDR-dependet

The predominant mechanistic effect of vitamin D is VDR-mediated induction or suppression of a large number of target genes. Yet, rapid, membrane-mediated effects of calcitriol have been described, which are mediated by calcitriol-induced calcium influx in target cells. For further mechanistic insights, we therefore assessed whether the antiviral effect of calcipotriol depends on VDR and / or on rapid calcium influx, respectively. As shown in Fig. 4A and B, silencing of VDR by siRNAs completely abrogated the antiviral effect of calcipotriol. In contrast, pre-treatment of human hepatoma cells with verapamil and U73122, two inhibitors of calcium influx into the cytosol from extracellular and intracellular stocks that were shown to block calcitriol-induced calcium influx[35], had no effect on the antiviral effect of calcipotriol (Fig. 4C). Furthermore, pre-treatment of human hepatoma cells with cycloheximide, an inhibitor of *de-novo* protein synthesis, abrogated the antiviral effect of calcipotriol, which further supports an

antiviral mechanism involving VDR-mediated gene expression and subsequent protein translation (Fig. 4D).

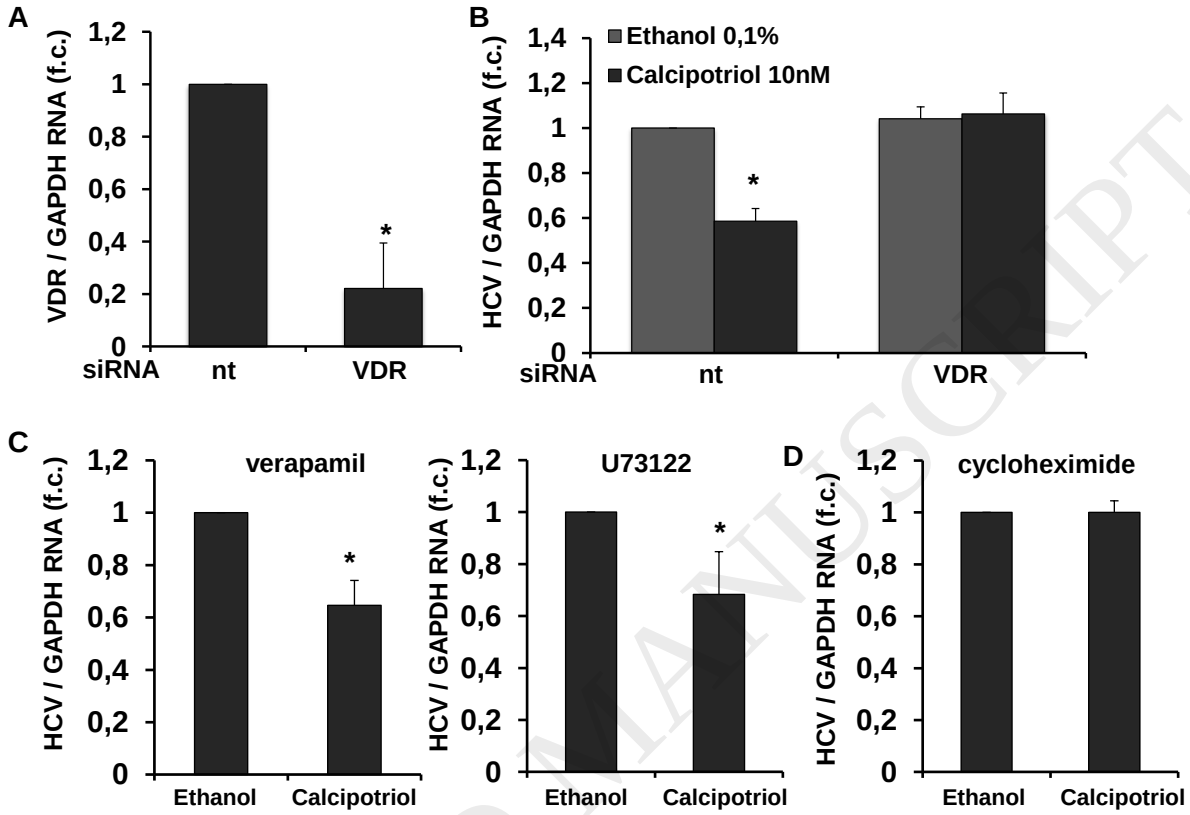

Fig. 4. The antiviral effect of calcipotriol depends on VDR. (A) Huh-7.5 cells harboring subgenomic HCV genotype 1b replicons were transfected with either non-targeting siRNA or siRNA #14799 tarteting VDR. After 72 hours, VDR silencing was confirmed by quantitative PCR (A), and cells were subsequently treated for 24 hours with mock (0.1% ethanol) or calcipotriol (B) to assess the impact on HCV replication by quantitative PCR. (C, D) Huh-7.5 cells harboring subgenomic HCV genotype 1b replicons were treated with calcipotriol for 24 hours after pre-treatment with 1 nM verapamil (C) or U73122 (D) for 2 hours followed by treatment with calcipotriol or mock. HCV RNA levels were measured by quantitative PCR. (D) Huh-7.5 cells harboring subgenomic HCV genotype 1b replicons were treated with calcipotriol for 24 hours after pre-treatment with cycloheximide (50 µg/µl) for 12 hours. HCV RNA levels relative to GAPDH mRNA were assessed after the 24 hours treatment period and expressed as

fold change (f.c.) relative to mock treated cells. Standard deviations of three independent experiments are shown. *$P < 0.05$.

3.3 Comparison of local topological features and bonding patterns between VDR-ligand binding domain structures bound to calcitriol or calcipotriol

Crystal structures of the VDR-ligand binding domain (LBD) bound to calcitriol (PDB-1DB1) or calcipotriol (PDB-1S19) are deposited in the Protein Databank RCSB PDB[27]. To picture structure rearrangements that are characteristic upon ligand binding, we made use of residue-interaction networks computed from the available experimental structure information (see Materials and Methods).

The network comparison view between VDR-ligand binding domain (LBD) structures bound to calcitriol (PDB-1DB1) or calcipotriol (PDB-1S19) shows direct ligand interaction to 24 neighboring residues (Figure 5). Among those interacting residues are sites that stabilize the VDR-LBD protein fold (residues 286, 295), as well as functional important sites that pertain to the (i) VDR-activation domain (residues 227, 230, 231, 233, 234, 237, 397, 422) and (ii) the charge clamp (residues 246, 420). By comparing binding of calcitriol *versus* calcipotriol to the VDR, we have observed a ligand-specific bonding pattern with residues of the VDR-activation domain, A231 and F422. The residue side chain-ligand interaction with F422 is unique in the VDR-calcitriol structure, whereas side chain-ligand and main chain-ligand interactions with A231 are specific for the VDR-calcipotriol structure. Additional specific van-der-Waals (vdW)-bondings in the two ligand-bound VDR structures (calcitriol *versus* calcipotriol) are identified between first neighbor residues 227-231, 232-233, 231-234, 232-275 and 231-418, that indicate distinct local structure rearrangements upon ligand binding (Figure 5 and SI Figure 1). In contrast, no specific H-bond interactions in the ligand-binding domain are observed between calcitriol and calcipotriol. Importantly, all vdW bondings that are distinct between

VDR-calcitriol and VDR-calcipotriol involve residues of the functional and structural important helix 3 (H3; 224-247) and helix 12 (H12; 416-422) with the exception of the interacting residue pair 272-275 that pertain to helix 4/5. The calcipotriol vdW-interaction with residue A231 is associated with an additional vdW interaction that arise between residues 231 and 418, the latter does not directly interact with any of the two ligands. Residue V418 is part of H12 and a direct neighbor of the H12-residue E420 that is part of the VDR-transactivation domain. Moreover, E420 together with K246 constitute the VDR-charge clamp that is essential for VDR-coactivator (CoA) or corepressor (CoR) binding[34]. In contrast to calcipotriol, another distinct bonding pattern and respective conformational rearrangement is observed for VDR-calcitriol that directly interact with the H12-residue F422. F422 is engaged in a cation-pi stacking interaction with H397 (SI Figure 1) that plays a key role in maintaining the stability of the H12 orientation and VDR-LBD conformation[34]. Importantly, calcipotriol has no direct contact with helix H12, whereas calcitriol shows direct H12-ligand interaction.

3.4 Putative ligand-induced molecular structural changes in the VDR-ligand binding domain

We found calcipotriol to induce changes in the non-covalent bonding pattern that affect residues of helix H3 (227, 231-234), whereas calcitriol directly interact with helix H12 (residue 418). The relative positioning of H3 and H12 and their impact on the VDR charge clamp are pivotal for agonistic, antagonistic or inverse agonistic protein conformations[29]. The positioning of H12 is reported to determine a critical distance in the charge clamp between its key residues K246 and E420[29, 34]. A ligand superposition (Figure 6B) showed calcipotriol with a side-chain cyclopropyl ring that in the protein structure PDB-1S19 is pointing away from H12, whereas in the calcitriol-bound structure PDB-1DB1 a respective aliphatic side chain is pointing towards the aromatic ring of F422 with a consecutive displacement of residue F422 in the VDR-

calcitriol *versus* VDR-calcipotriol structure (Figure 5, 6B and SI Figure 1). Thereby the F422 side-chain orientation is likely to impact the conformation of the neighboring H12-residue E420 and subsequently the VDR-charge clamp (Figure 5 and 6A, SI. Figure 1). Consecutive displacement of H12 is known to impact the binding of VDR to CoAs that explain partial agonist or full antagonist activity of ligands based on the length and structure of the respective side-chain extensions[36, 37].

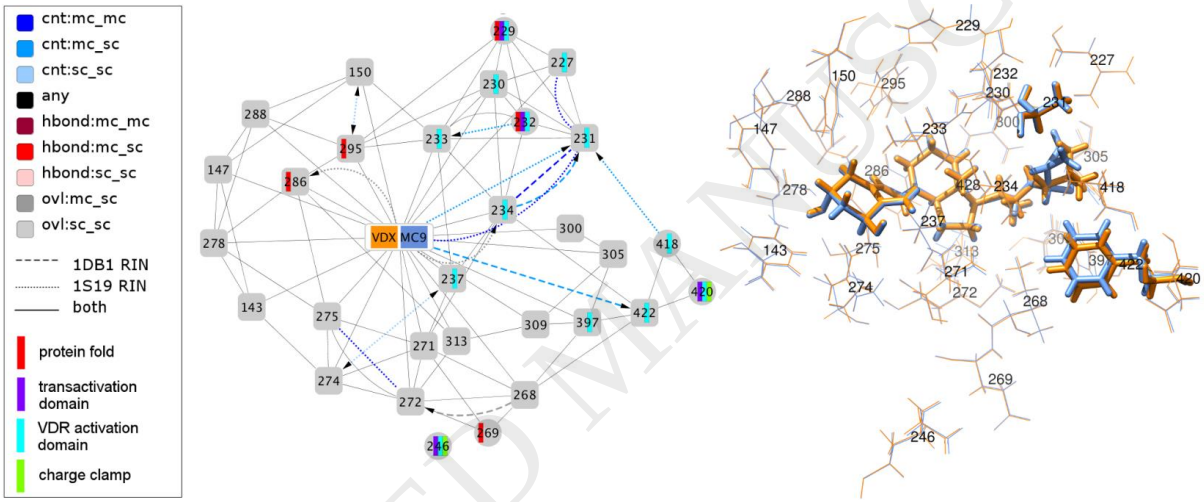

Figure 5. Comparison residue network and corresponding 3D structure close-up view on the ligand-binding site between VDR-calcitriol and VDR-calcipotriol. The comparison network view between VDR-calcitriol (PDB-1DB1; ligand: VDX) and VDR-calcipotriol (PDB-1S19; ligand: MCP) focuses on direct non-covalent interactions between ligands and first neighbours. The corresponding residues in the structure are shown as orange (VDR-calcitriol) and blue sticks (VDR-calcipotriol, respectively. Structure or functionally important sites are indicated by colored bars within the residue network (see legend on the left).

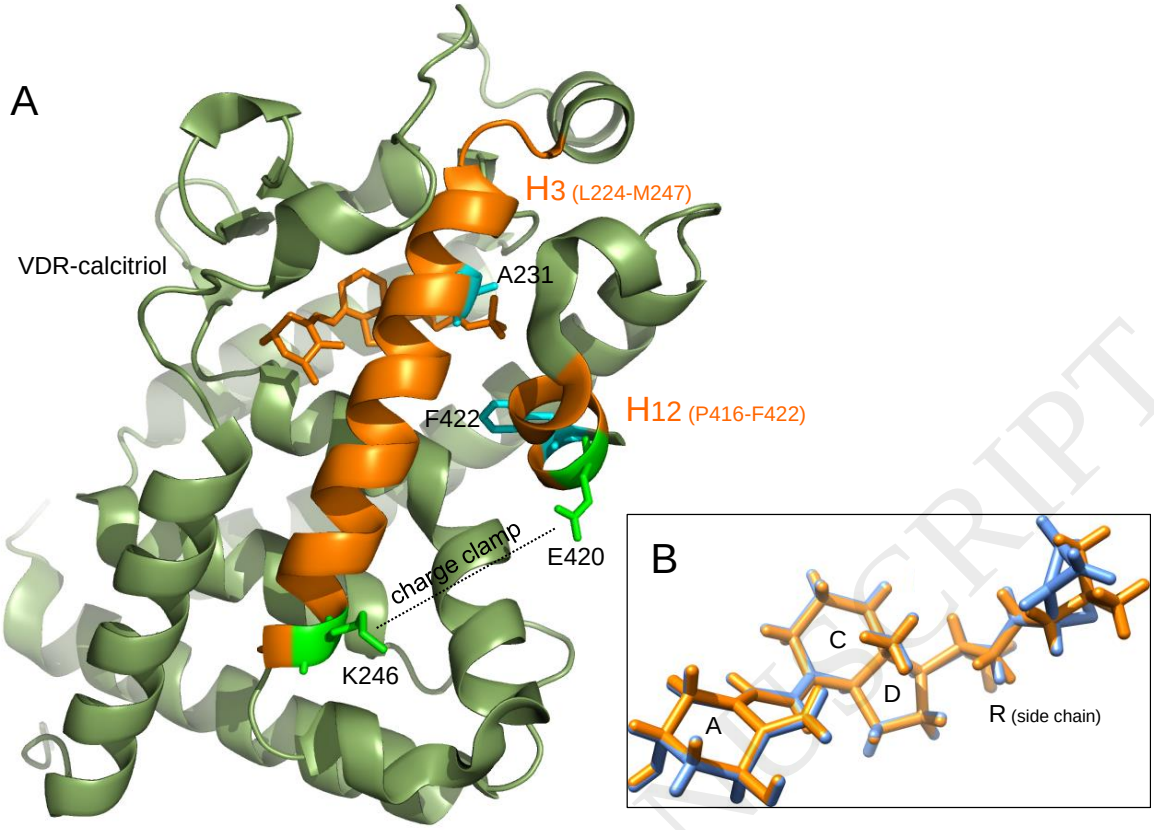

Figure 6. 3D protein structure of the VDR-LBD. (A) The protein structure shows the VDR-LBD from PDB entry 1DB1 co-crystallized with calcitriol (orange stick model). The protein backbone is given as ribbon model with functionally important residues depicted as stick models. Helix 3 and 12 are highlighted in orange. (B) Ligand superposition of calcitriol (orange) and calcipotriol (blue) from PDB entry 1DB1 and 1S19 respectively.

3.5 Differential impact of calcipotriol versus calcitriol on the hepatocellular transcriptome

The above described differential interactions of calcipotriol *vs*. calcitriol with key regulatory residues of the VDR suggest rather broad than selective consequences on VDR-regulated gene expression (i.e. affecting multiple rather than single genes). To test this hypothesis, we performed micro-array analyses to investigate the impact of calcipotriol *vs.* calcitriol on the hepatocellular transcriptome. As shown in Fig. 7A, transcriptome profiles of human hepatoma cell lines stimulated for 12 hours with calcipotriol differed from those stimulated with calcitriol. Namely, calcipotriol appeared to have a stronger, but also broader impact on the hepatocellular gene expression (SI Table 1). Furthermore, the effect of calcipotriol appeared to be more consistant than that of calcitriol, probably because the lower efficacy of calcitriol to induce/repress hepatocellular VDR target genes results in higher stochastic variation of gene expression (Fig. 7A). Quantitative PCR confirmed that calcipotriol results in a stronger induction of a number of selected target genes (Fig. 7). Furthermore, exposure of human hepatoma cell lines to low doses of calcipotriol resulted in a faster induction of *CYP24A1* – an important target gene of the VDR regulating the bioavailability of calcitriol[8] – compared to calcitriol, although at high doses calcitriol was equally effective in inducing *CYP24A1* than calcipotriol.

To set our findings in a broader context, we next assessed the effect of calcipotriol *versus* calcitriol on gene expression of two functionally highly relevant innate immune VDR target genes, cathelicidin and hepcidin, in macrophages, a key target cell type of vitamin D-mediated immune regulation[38, 39]. Calthelicidin is a well-known target gene of the VDR with potent anti-mycobacterial, antibacterial and antiviral properties[39]. Hepcidin is a key regulator of iron metabolism and has pleiotropic antibacterial effects[40]. The presence of VDR in THP1 cell lines and MDMs was confirmed by Western blot analyses (Fig. 8A). As shown in Fig. 8B, calcipotriol has an equally directed, though significantly stronger effect on cathelicidin-

induction and hepcidin-repression than calcitriol in human macrophage-like THP-1-cells or primary human macrophages.

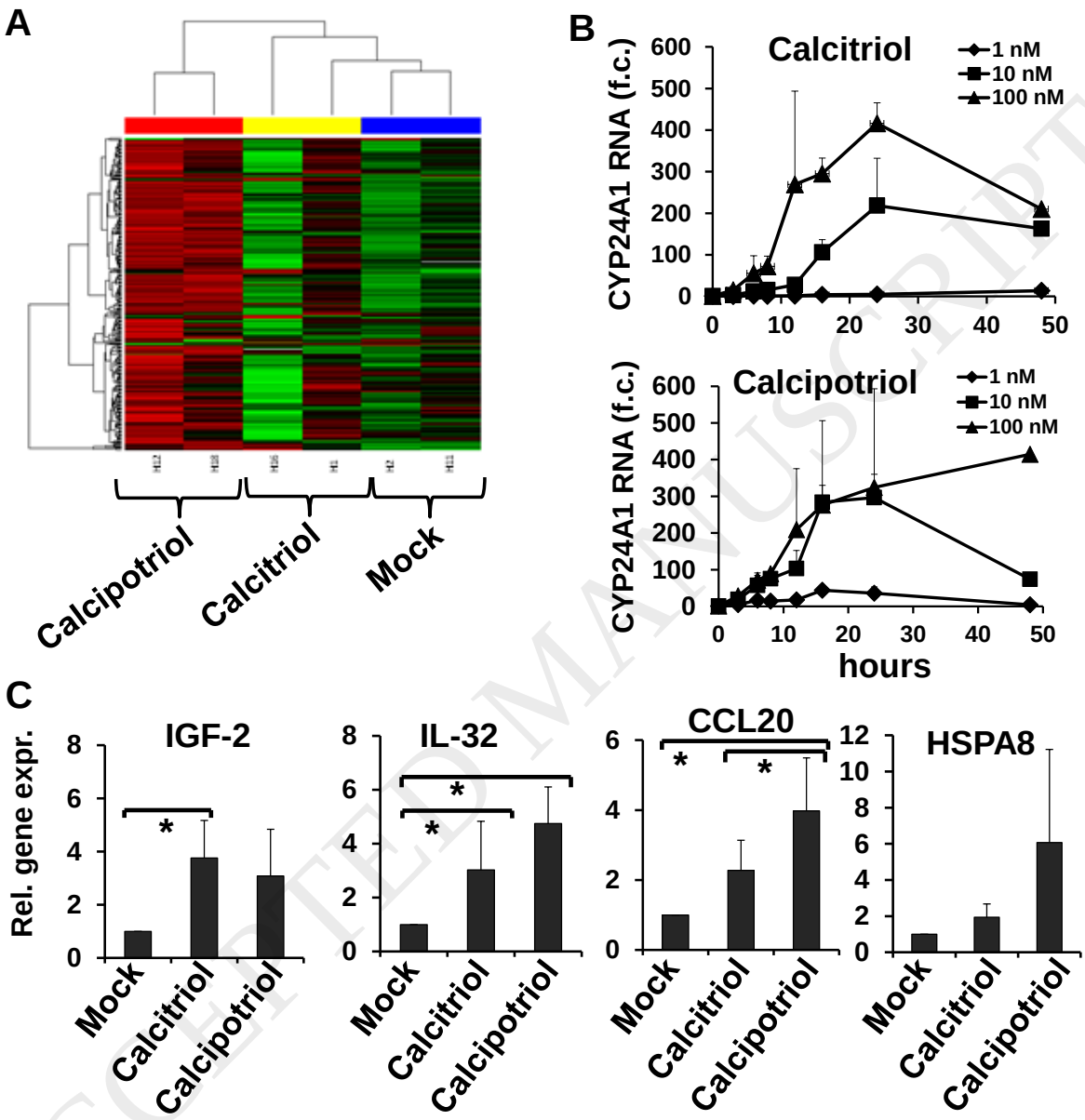

Fig. 7 Differential impact of calcipotriol versus calcitriol on the hepatocellular transcriptome. (A) Unsupervised hierarchical clustering (300 Probesets with the highest standard deviation) of Huh-7.5 cells treated with calcipotriol, calcitriol or mock (0.1% ethanol). Heat map of Huh-7.5 cells treated with 10 nM of calcipotriol, 10 nM of calcitriol, or mock for 12 hours. (B) Huh-7.5 cells harboring subgenomic HCV genotype 1b replicons were stimulated

with 1, 10 and 100 nM of calcitriol and calcipotriol for 3, 6, 8, 12, 24 and 48 hours. CYP24A1 mRNA levels normalized to GAPDH mRNA are expressed relative to mock (0.1% ethanol) treated cells. (C) Huh-7.5 cells were treated with 10 nM calcitriol and calciptriol for 16h. IGF-2, IL-32, CCL20 and HSPA8 mRNA levels normalized to GAPDH mRNA are expressed relative to mock treated cells. Standard deviations of three independent experiments are shown. f.c., fold change. *P<0.05.

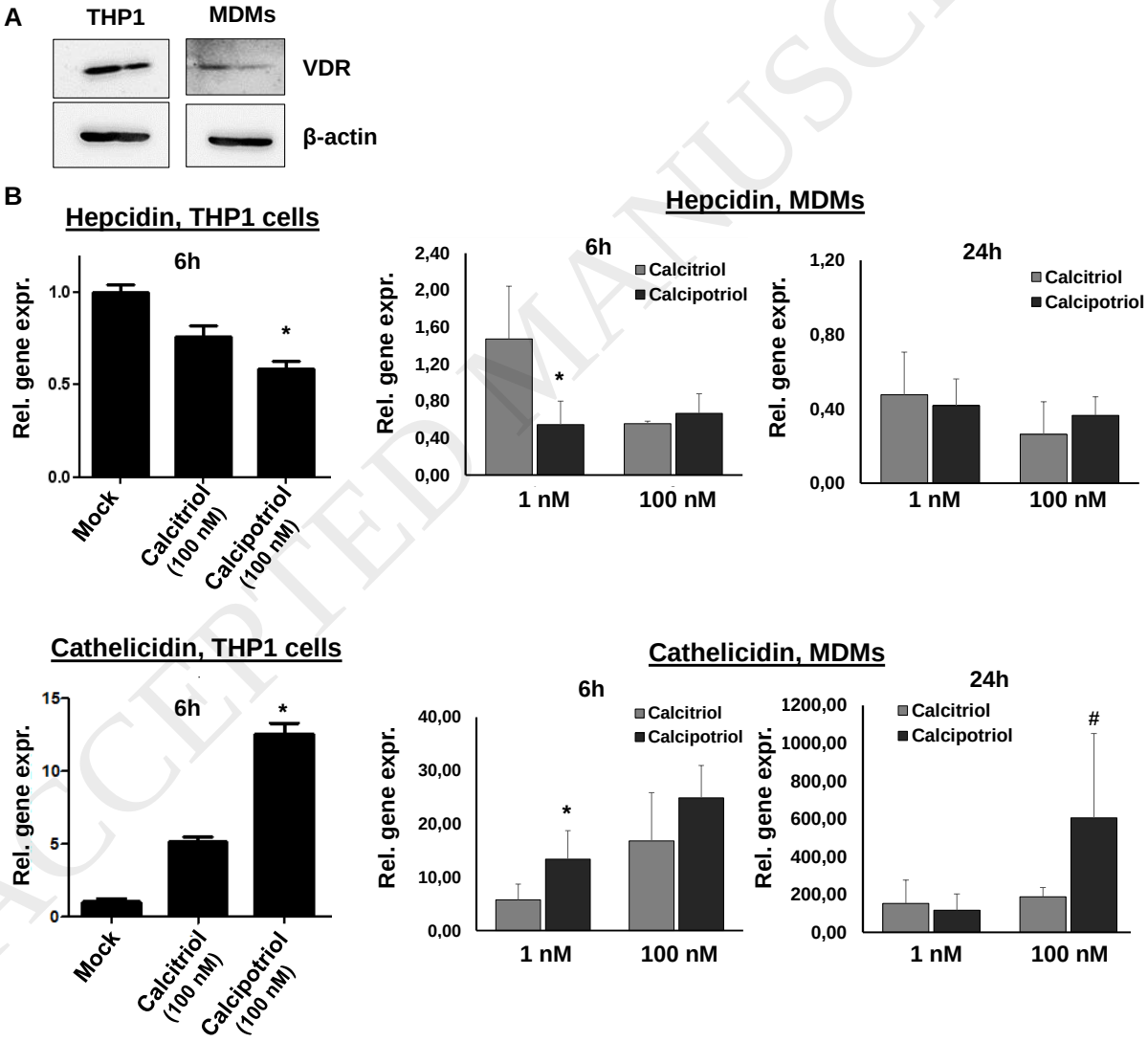

Fig. 8. Calcipotriol is a regulator of cathelicidin and hepcidin gene expression. (A) Two independent cell lysates each of THP1 cell lines or MDMs were analyzed by Western blot for protein

levels of VDR and β-actin. (B) THP-1 cell lines, treated with 50 nmol/mL PMA for 72 hours to differentiate them into a macrophage-like phenotype, or primary human myeloid-derived macrophages (MDMs) were stimulated with calcitriol or calcipotriol for the indicated time points. Relative mRNA levels of cathelicidin or hepcidin are shown for three independent experiments. *P<0.05; #P<0.1.

4 Discussion

In the present study we show that the synthetical calcitriol-derivative calcipotriol, but not calcitriol itself, inhibits HCV replication, and has a superior capacity to induce a number of VDR target genes in hepatocytes and macrophages as compared to calcitriol. These target genes include important effectors of innate immune responses such as hepcidin and cathelicidin[38-41]. Mechanistically, we show distinct interactions of calcipotriol with important regulatory modules of the VDR that seem to result in differential interaction with VDR corepressors and -activators that translate into different transcriptomic profiles and immune responses in target cells.

Topical calcipotriol is an important first-line agent for the treatment of psoriasis with a superior efficacy and risk profile compared for example to topical steroids [42]. The beneficial effects of calcipotriol in psoriasis are explained by regulation of keratinocyte differentiation and inhibition of pathogenic Th17 cells, though these phenomena are incompletely understood [42]. Additional emerging examples of a possible clinical usage of calcipotriol are immunotherapy of skin cancer precursor lesions, or the discovery of a VDR / SMAD genomic circuit, in which ligand-binding of calcipotriol to VDR inhibits TGF-β-driven liver fibrosis [43, 44]. Our study extends this spectrum by showing that monotherapy with calcipotriol, but not with calcitriol, inhibits replication of hepatitis C virus *in vitro*, which might be explained by increased

expression / repression of innate immune VDR target genes in the liver. Overall, our and the above summarized data support the evaluation of calcipotriol as an agent for systemic therapy (so far, calcipotriol was only approved for topical therapy) of diseases like hepatitis C which may be susceptible for VDR signaling. This hypothesis is further supported by the fact that calcipotriol has little effects on serum calcium levels in contrast to calcitriol, and may therefore be administered at significantly higher doses than calcitriol. In fact, hypercalcemia limits the utility of calcitriol to therapeutically execute non-classical vitamin D effects, which would require supraphysiological doses of calcitriol.

The generally accepted and here – with respect to inhibition of HCV – further elaborated superior capacity of calcipotriol to mediate non-classical (i.e. beyond calcium homeostasis) vitamin D effects are mechanistically incompletely understood, as both agents appear to bind to the VDR with comparable affinities. The molecular differences between calcitriol and calcipotriol (as well as between other calcitriol-analogs) are very subtle, but ligand-triggered VDR-protein interactions are central to VDR function with only one agonistic conformation of the VDR-LBD[34]. Central to this conformation is a residue interaction of H397 with F422 forming a bridge to stabilize H12 conformation with respect to the VDR "charge clamp"[34]. In the present study we reveal a residue network characterized by distinct conformational changes due to VDR-clacitriol versus –calcipotriol binding that affect the local conformation of those residues. The charge clamp again provides optimal positioning to interact with CoA proteins. Superagonistic ligands like calcipotriol may increase the affinity of CoAs due to their impact on H397 and/or F422. In additional co-immunoprecipitation experiments we could provide preliminary *in vitro* evidence supporting this notion (i.e. stronger binding of VDR to SRC1 in the presence of calcipotriol *versus* calcitriol); however these results should be considered as preliminary due to (presumably technical) difficulties to perform these co-immunoprecipitation

experiments (SI Figure 2). Importantly, specific small molecule inhibitors of the interactions between the VDR and CoAs have recently been developed, which may further increase the future therapeutic arsenal to treat diseases in which VDR signaling is involved[45].

Our study has important limitations. Most importantly, we were not able to identify the underlying mechanism of how calcipotriol inhibits HCV replication. Furthermore, future studies are warranted to assess whether the superior induction of innate immune genes like cathelicidine by calcipotriol in contrast to calcitriol translates effectively into a superior clinical profile of calcipotriol versus calcitriol.

Collectively, our data reveal subtle structural differences of calcipotriol *versus* calcitriol resulting in distinctive interactions with decisive regulatory residues of the VDR. These appear to translate in a superior clinical potential of calcipotriol to execute important non-classical vitamin D effects such as inhibition of HCV replication and on innate immune regulation.

Authors' contributions. The authors have contributed to the manuscript by planning the study (CW, JG, KH, CS, KB, DM, SZ, CML), collecting the data (MS, CW, CC, JF, KH, CD, CS, SR, CML), analyzing data (MS, CW, CC, JG, JF, KH, CD, CS, KB, DM, SZ, SR, CML), and preparing as well as revising the manuscript (all authors).

Acknowledgements. The authors express their gratitude to Ralf Bartenschlager, Charles M. Rice, Klaus Roemer, and Nicolas Mitsiades for reagents, to Yolanda Martinez for expert technical assistance, and to Rolf Marschalek for helpful discussions. We thank Nadezhda T. Doncheva for assistance with the residue network figures.

Financial support. This study was supported by the Else Kröner-Fresenius-Stiftung (2013_A165 to CML), the Deutsche Forschungsgemeinschaft (LA 2806/2-1 and LA 2806/5-1 to CML), and by the LOEWE Zentrum Druid (to CML and SZ). MS received a scholarship funded by the Egyptian Ministry of Higher Education and the German Academic Exchange Service (DAAD). CW was supported by the GILEAD Sciences International Research Scholars Program in Liver Disease and the Deutsche Forschungsgemeinschaft (WE 4388/6-1).

Conflicts of interest. None.

5 References

1. Assa A, Vong L, Pinnell LJ, et al. Vitamin D deficiency promotes epithelial barrier dysfunction and intestinal inflammation. J Infect Dis 2014;210:1296-305.
2. Lange CM, Bibert S, Dufour JF, et al. Comparative genetic analyses point to HCP5 as susceptibility locus for HCV-associated hepatocellular carcinoma. J Hepatol 2013;59:504-9.
3. Lange CM, Bojunga J, Ramos-Lopez E, et al. Vitamin D deficiency and a CYP27B1-1260 promoter polymorphism are associated with chronic hepatitis C and poor response to interferon-alfa based therapy. J Hepatol 2011;54:887-93.
4. Lee P, Eisman JA, Center JR. Vitamin D deficiency in critically ill patients. N Engl J Med 2009;360:1912-4.
5. Levin GP, Robinson-Cohen C, de Boer IH, et al. Genetic variants and associations of 25-hydroxyvitamin D concentrations with major clinical outcomes. JAMA 2012;308:1898-905.
6. Petta S, Camma C, Scazzone C, et al. Low vitamin D serum level is related to severe fibrosis and low responsiveness to interferon-based therapy in genotype 1 chronic hepatitis C. Hepatology 2010;51:1158-67.
7. Farnik H, Bojunga J, Berger A, et al. Low vitamin D serum concentration is associated with high levels of hepatitis B virus replication in chronically infected patients. Hepatology 2013;58:1270-6.
8. Campbell FC, Xu H, El-Tanani M, et al. The yin and yang of vitamin D receptor (VDR) signaling in neoplastic progression: operational networks and tissue-specific growth control. Biochem Pharmacol 2010;79:1-9.
9. Ramagopalan SV, Heger A, Berlanga AJ, et al. A ChiP-seq defined genome-wide map of vitamin D receptor binding: Associations with disease and evolution. Genome Research 2010;20:1352-60.
10. von Essen MR, Kongsbak M, Schjerling P, et al. Vitamin D controls T cell antigen receptor signaling and activation of human T cells. Nat Immunol 2010;11:344-9.
11. Martineau AR, Jolliffe DA, Hooper RL, et al. Vitamin D supplementation to prevent acute respiratory tract infections: systematic review and meta-analysis of individual participant data. BMJ 2017;356:i6583.
12. Martineau AR, Timms PM, Bothamley GH, et al. High-dose vitamin D(3) during intensive-phase antimicrobial treatment of pulmonary tuberculosis: a double-blind randomised controlled trial. Lancet 2011;377:242-50.
13. Leyssens C, Verlinden L, Verstuyf A. The future of vitamin D analogs. Front Physiol 2014;5:122.
14. Eelen G, Verlinden L, Rochel N, et al. Superagonistic action of 14-epi-analogs of 1,25-dihydroxyvitamin D explained by vitamin D receptor-coactivator interaction. Mol Pharmacol 2005;67:1566-73.
15. Yamamoto H, Shevde NK, Warrier A, et al. 2-Methylene-19-nor-(20S)-1,25-dihydroxyvitamin D3 potently stimulates gene-specific DNA binding of the vitamin D receptor in osteoblasts. J Biol Chem 2003;278:31756-65.
16. Holick MF. Vitamin D deficiency. N Engl J Med 2007;357:266-81.
17. Rosen CJ. Clinical practice. Vitamin D insufficiency. N Engl J Med 2011;364:248-54.
18. de Zeeuw D, Agarwal R, Amdahl M, et al. Selective vitamin D receptor activation with paricalcitol for reduction of albuminuria in patients with type 2 diabetes (VITAL study): a randomised controlled trial. Lancet 2010;376:1543-51.

19. Lange CM, Gouttenoire J, Duong FH, et al. Vitamin D receptor and Jak-STAT signaling crosstalk results in calcitriol-mediated increase of hepatocellular response to IFN-alpha. J Immunol 2014;192:6037-44.
20. Blight KJ, Kolykhalov AA, Rice CM. Efficient initiation of HCV RNA replication in cell culture. Science 2000;290:1972-4.
21. Wakita T, Pietschmann T, Kato T, et al. Production of infectious hepatitis C virus in tissue culture from a cloned viral genome. Nat Med 2005;11:791-6.
22. Heyne K, Heil TC, Bette B, et al. MDM2 binds and inhibits vitamin D receptor. Cell Cycle 2015;14:2003-10.
23. Geng C, He B, Xu L, et al. Prostate cancer-associated mutations in speckle-type POZ protein (SPOP) regulate steroid receptor coactivator 3 protein turnover. Proc Natl Acad Sci U S A 2013;110:6997-7002.
24. Bellecave P, Sarasin-Filipowicz M, Donze O, et al. Cleavage of mitochondrial antiviral signaling protein in the liver of patients with chronic hepatitis C correlates with a reduced activation of the endogenous interferon system. Hepatology 2010;51:1127-36.
25. Rengstl B, Schmid F, Weiser C, et al. Tumor-infiltrating HLA-matched CD4(+) T cells retargeted against Hodgkin and Reed-Sternberg cells. Oncoimmunology 2016;5:e1160186.
26. Moradpour D, Bieck E, Hugle T, et al. Functional properties of a monoclonal antibody inhibiting the hepatitis C virus RNA-dependent RNA polymerase. J Biol Chem 2002;277:593-601.
27. Rose PW, Bi C, Bluhm WF, et al. The RCSB Protein Data Bank: new resources for research and education. Nucleic Acids Res 2013;41:D475-82.
28. Rochel N, Wurtz JM, Mitschler A, et al. The crystal structure of the nuclear receptor for vitamin D bound to its natural ligand. Mol Cell 2000;5:173-9.
29. Tocchini-Valentini G, Rochel N, Wurtz JM, et al. Crystal structures of the vitamin D nuclear receptor liganded with the vitamin D side chain analogues calcipotriol and seocalcitol, receptor agonists of clinical importance. Insights into a structural basis for the switching of calcipotriol to a receptor antagonist by further side chain modification. J Med Chem 2004;47:1956-61.
30. Doncheva NT, Klein K, Domingues FS, et al. Analyzing and visualizing residue networks of protein structures. Trends Biochem Sci 2011;36:179-82.
31. Word JM, Lovell SC, Richardson JS, et al. Asparagine and glutamine: using hydrogen atom contacts in the choice of side-chain amide orientation. J Mol Biol 1999;285:1735-47.
32. Word JM, Lovell SC, LaBean TH, et al. Visualizing and quantifying molecular goodness-of-fit: small-probe contact dots with explicit hydrogen atoms. J Mol Biol 1999;285:1711-33.
33. Doncheva NT, Klein K, Morris JH, et al. Integrative visual analysis of protein sequence mutations. BMC Proc 2014;8:S2.
34. Wan LY, Zhang YQ, Chen MD, et al. Relationship between Structure and Conformational Change of the Vitamin D Receptor Ligand Binding Domain in 1alpha,25-Dihydroxyvitamin D3 Signaling. Molecules 2015;20:20473-86.
35. Doroudi M, Schwartz Z, Boyan BD. Membrane-mediated actions of 1,25-dihydroxy vitamin D3: a review of the roles of phospholipase A2 activating protein and Ca(2+)/calmodulin-dependent protein kinase II. J Steroid Biochem Mol Biol 2015;147:81-4.
36. Herdick M, Steinmeyer A, Carlberg C. Carboxylic ester antagonists of 1alpha,25-dihydroxyvitamin D(3) show cell-specific actions. Chem Biol 2000;7:885-94.

37. Ishizuka S, Miura D, Ozono K, et al. Antagonistic Actions in Vivo of (23S)-25-Dehydro-1alpha-Hydroxyvitamin D(3-)26,23-Lactone on Calcium Metabolism Induced by 1alpha,25-Dihydroxyvitamin D(3). Endocrinology 2001;142:59-67.
38. Bacchetta J, Zaritsky JJ, Sea JL, et al. Suppression of iron-regulatory hepcidin by vitamin D. J Am Soc Nephrol 2014;25:564-72.
39. Liu PT, Stenger S, Li H, et al. Toll-like receptor triggering of a vitamin D-mediated human antimicrobial response. Science 2006;311:1770-3.
40. Michels K, Nemeth E, Ganz T, et al. Hepcidin and Host Defense against Infectious Diseases. PLoS Pathog 2015;11:e1004998.
41. Bartolomei G, Cevik RE, Marcello A. Modulation of hepatitis C virus replication by iron and hepcidin in Huh7 hepatocytes. J Gen Virol 2011;92:2072-81.
42. Kim GK. The rationale behind topical vitamin d analogs in the treatment of psoriasis: where does topical calcitriol fit in? J Clin Aesthet Dermatol 2010;3:46-53.
43. Ding N, Yu RT, Subramaniam N, et al. A vitamin D receptor/SMAD genomic circuit gates hepatic fibrotic response. Cell 2013;153:601-13.
44. Cunningham TJ, Tabacchi M, Eliane JP, et al. Randomized trial of calcipotriol combined with 5-fluorouracil for skin cancer precursor immunotherapy. J Clin Invest 2017;127:106-116.
45. Nandhikonda P, Lynt WZ, McCallum MM, et al. Discovery of the first irreversible small molecule inhibitors of the interaction between the vitamin D receptor and coactivators. J Med Chem 2012;55:4640-51.